Article

Bonding and Oxidation State of a Transition Metal Atom Encapsulated in an Isolated Octahedral Cluster Cation of Main Group Elements: Synthesis, Crystal Structure, and Electronic Structure of $PtIn_8GaOF^-$ Containing Highly Positive 18-Electron Complex $[PtIn]^+$ and Low-Valent In Ions

Jrgen Khler, Jen-Hui Chang, and Myung-Hwan Whangbo

J. Am. Chem. Soc., **2005**, 127 (7), 2277-2284• DOI: 10.1021/ja044389s • Publication Date (Web): 25 January 2005

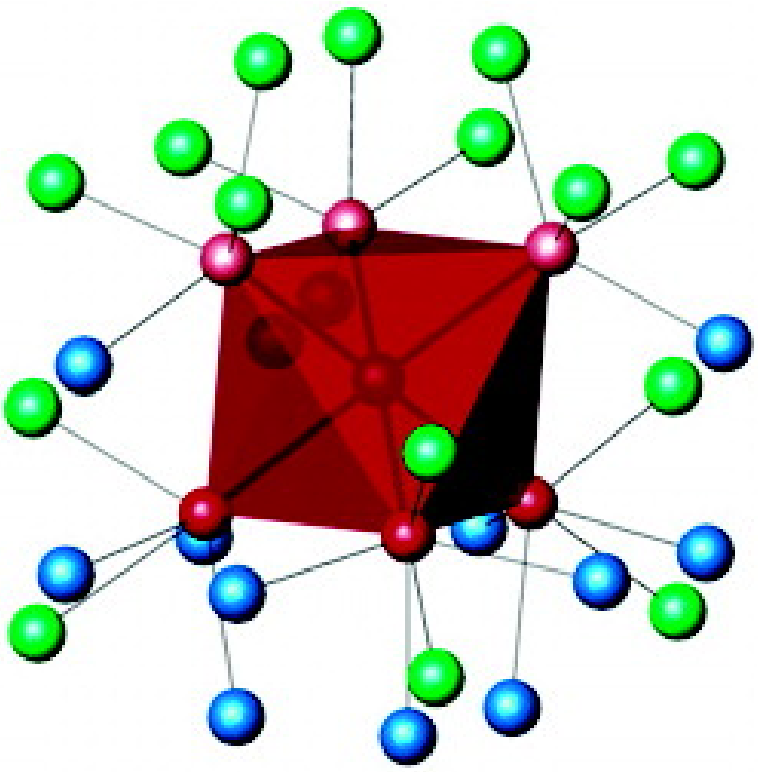

More About This Article

Additional resources and features associated with this article are available within the HTML version:

- Supporting Information
- Links to the 9 articles that cite this article, as of the time of this article download

J|A|C|S
ARTICLES
Published on Web 01/25/2005

Bonding and Oxidation State of a Transition Metal Atom Encapsulated in an Isolated Octahedral Cluster Cation of Main Group Elements: Synthesis, Crystal Structure, and Electronic Structure of $Pt_2In_{14}Ga_3O_8F_{15}$ Containing Highly Positive 18-Electron Complex $[PtIn_6]^{10+}$ and Low-Valent In^+ Ions

Jürgen Köhler,*,† Jen-Hui Chang,† and Myung-Hwan Whangbo*,‡

Contribution from the Max-Planck-Institut für Festkörperforschung, Stuttgart, Germany, and Department of Chemistry, North Carolina State University, Raleigh, North Carolina 27695-8204

Received September 15, 2004; E-mail: j.koehler@fkf.mpg.de; mike_whangbo@ncsu.edu

Abstract: Colorless transparent single crystals and white polycrystalline powder samples of $Pt_2In_{14}Ga_3O_8F_{15}$ were obtained by heating a mixture of stoichiometric amounts of Pt, In, InF_3, and Ga_2O_3, in a Pt crucible under Ar at 600 °C. The new oxyfluoride crystallizes in a new structure type in the trigonal space group $R\bar{3}m$ (No. 166) with $a = 709.0(6)$ pm, $c = 4556.4(3)$ pm, and $Z = 6$ with characteristic building units of $PtIn_6$ octahedra (Pt−In = 255−257 pm), GaF_6 octahedra (Ga−F = 189 pm), and GaO_4 tetrahedra (Ga−O = 186−187 pm). This oxyfluoride consists of a highly positive 18-electron complex $[PtIn_6]^{10+}$ as well as low-valent In^+ ions. Electronic band structure calculations for $Pt_2In_{14}Ga_3O_8F_{15}$ and molecular orbital (MO) calculations for $[PtIn_6]^{10+}$ were carried out to analyze the electronic structure of $[PtIn_6]^{10+}$ and estimate the oxidation state of Pt. Our analysis indicates that the oxidation state of the Pt atom in $[PtIn_6]^{10+}$ is negative rather than positive. For other octahedral cluster cations of main group elements stuffed with a transition metal atom (e.g., $[RuSn_6]^{14+}$ and "$[IrBi_6]^{11+}$") as well, we showed that the oxidation state of the transition metal atom is most probably negative by studying their electronic structures.

1. Introduction

There are several kinds of interesting octahedral cluster compounds. Some halides and chalcogenides have octahedral clusters made up of transition metal atoms,[1,2] while some oxides and halides have octahedral clusters of main group elements that are stuffed with a transition metal atom, e.g., $RuSn_6$ in $Ru_3Sn_{15}O_{14}$[3] and $RuSn_6[(Al_{(1/3)-x}Si_{3x/4})O_4]_2$ ($0 \le x \le 1/3$),[4] $PtIn_6$ in $PtIn_6(GaO_4)_2$,[5] and $IrBi_6$ in $Bi_{34}Ir_3Br_{37}$.[6] The compounds $K_{10}In_{10}M$ (M = Ni, Pd, Pt)[7] consist of isolated MIn_{10} clusters in which each transition metal M is encapsulated in the distorted, tetracapped trigonal prism In_{10}. Some halides have octahedral clusters of rare-earth elements stuffed with a transition metal atom, e.g., $OsPr_6$ in $Cs_4Pr_6OsI_{13}$[8] and $K_4Pr_6I_{14}Os$[9a] and $OsLa_6$ in $K_4La_6OsI_{14}$.[9b] Similar cluster compounds containing fluoride ions are difficult to obtain because volatile compounds are formed during synthesis and because, compared with phases containing metals in high oxidation states, reduced phases are much less stable.[10] Therefore, it is not surprising that Nb_6F_{15}[11] had been the only known fluoride-containing metal clusters for a long time, and other examples such as $PtIn_7F_{13}$[12] and $Pt_3In_{22}F_{40}$,[13] which contain $PtIn_6$ octahedral clusters found in $PtIn_6Ga_2O_8$, have been discovered only recently. Our effort to prepare an oxyfluoride containing the elements Pt and In has led to a new-phase $Pt_2In_{14}Ga_3O_8F_{15}$ that has not only low-valent In^+ ions but also highly positive $[PtIn_6]^{10+}$ ions as found in $PtIn_6Ga_2O_8$, $PtIn_7F_{13}$, and $Pt_3In_{22}F_{40}$. In the present work, we first describe the synthesis and the crystal structure determination of $Pt_2In_{14}Ga_3O_8F_{15}$ and then analyze the electronic structure of $Pt_2In_{14}Ga_3O_8F_{15}$ and that of the $[PtIn_6]^{10+}$ cation to find that the Pt atom of the highly positive cation $[PtIn_6]^{10+}$ has a negative oxidation state rather than a positive oxidation state. For other highly positive octahedral cluster cations of main group elements stuffed with a transition metal atom, we show that the transition metal atom most probably has a negative oxidation state by investigating the electronic structures of the $[RuSn_6]^{14+}$ cation

† Max-Planck-Institut für Festkörperforschung.
‡ North Carolina State University.

(1) Simon, A. *Angew. Chem.* **1981**, *93*, 23; *Angew. Chem., Int. Ed. Engl.* **1981**, *20*, 1.
(2) (a) McCarley, R. E.; Lii, K.-H.; Edwards, P. A.; Brough, L. F. *J. Solid State Chem.* **1985**, *57*, 17. (b) Köhler, J.; Svensson, G.; Simon, A. *Angew. Chem.* **1992**, *104*, 1463; *Angew. Chem., Int. Ed. Eng.* **1992**, *31*, 1437. (c) Köhler, J.; Svensson, G.; Simon, A. *Angew. Chem.* **1992**, *104*, 1463; *Angew. Chem., Int. Ed. Eng.* **1992**, *31*, 1437.
(3) Reichelt, W.; Söhnel, T.; Rademacher, O.; Oppermann, H.; Simon, A.; Mattausch, Hj.; Köhler, J. *Angew. Chem.* **1995**, *107*, 2307; *Angew. Chem., Int. Ed. Engl.* **1995**, *34*, 2113.
(4) Söhnel, T.; Reichelt, W.; Wagner, F. E. *Z. Anorg. Allg. Chem.* **2000**, *626*, 223.
(5) Friedrich, H. A.; Köhler, J. *Z. Anorg. Allg. Chem.* **2001**, *627*, 144.
(6) Ruck, M. *Z. Anorg. Allg. Chem.* **1998**, *624*, 521.
(7) Sevov, S, C.; Corbett, J. D. *J. Am. Chem. Soc.* **1993**, *115*, 9089.
(8) Lulei, M.; Corbett, J. D. *Inorg. Chem.* **1996**, *35*, 4084.
(9) (a) Uma, S.; Martin, J. D.; Corbett, J. D. *Inorg. Chem.* **1999**, *38*, 3825. (b) Uma, S.; Corbett, J. D. *Inorg. Chem.* **1999**, *38*, 3831.
(10) Johnson, D. A. *Some Thermodynamic Aspects of Inorganic Chemistry*, 2nd ed.; Cambridge University Press: Cambridge, U.K., 1982.
(11) Schäfer, H.; Schnering, H. G. v.; Niehues, K. J.; Nieder-Vahrenholz, H. G. *J. Less-Common Met.* **1965**, *9*, 95.
(12) Köhler, J.; Chang, J.-H. *Angew. Chem.* **2000**, *112*, 2077; *Angew. Chem., Int. Ed.* **2000**, *39*, 1998.
(13) Köhler, J.; Chang, J.-H. *5. Jahrestag. DGK, Referateband* **1997**, 12.

of $RuSn_6[(Al_{1/3-x}Si_{3x/4})O_4]_2$ and the "$[IrBi_6]^{11+}$" cation reported to be present in $Bi_{34}Ir_3Br_{37}$, which consists of three $IrBi_6$ octahedra, one Bi_6 octahedron, and two Bi_5 square pyramids per formula unit.

2. Experimental Section

2.1. Synthesis. Carefully dried InF_3 (p.a. Merck) was first mixed with Pt powder (p.a. Merck), In powder (Alfa, 99.99%, 325 mesh), and Ga_2O_3 (Alfa, 99.99%) in stoichiometric amounts. The mixture was ground in an agate mortar to a gray colored powder under Ar. Then the powder was pressed to a pellet, sealed under Ar in a Pt tube, and heated for 14 days at 600 °C. After cooling to room temperature (1°/min), colorless transparent crystals of $Pt_2In_{14}Ga_3O_8F_{15}$ with a platelike trigonal habit were found. Pure powder samples of $Pt_2In_{14}Ga_3O_8F_{15}$ were obtained by heating the pellets at 600 °C for 3 days, cooling to room temperature, grinding again, pressing a pellet, and heating for another 3 days at 600 °C. $Pt_2In_{14}Ga_3O_8F_{15}$ is stable in air and insoluble in diluted HCl.

The elemental analysis of a powder sample of $Pt_2In_{14}Ga_3O_8F_{15}$ with ICP [14] gave a Pt/In/Ga ratio of 2.0(1):14.0(1):2.9(1). For the determination of the O/F content, wavelength-dispersive X-ray (WDX) analyses were performed on a single crystal of $Pt_2In_{14}Ga_3O_8F_{15}$. The result (4.6 mol % Pt, 34.9 mol % In, 7.0 mol % Ga, 18.7 mol % O, and 34.8 mol % F) is in excellent agreement with the formula $Pt_2In_{14}Ga_3O_8F_{15}$ especially concerning the O/F ratio of 8:15. Standard deviations for the WDX analysis cannot be given because they depend on the atomic weights of the elements and the orientation of the crystal. Standard deviations can be estimated only when similar compounds with known corresponding element ratios and crystal orientation are measured for comparison.

2.2. Structure Determination. The single-crystal X-ray investigation was performed on a four-circle diffractometer (CAD4, Nonius) using Ag Kα radiation (graphite monochromator). The intensities were corrected for Lorentz and polarization effects, and a semiempirical absorption correction was applied on the basis of ψ-scans. Table S1 summarizes the crystallographic characteristics and the experimental conditions of the data collection and refinement. All calculations were performed using SHELX programs.[15,16] Atomic scattering factors and anomalous dispersion corrections were taken from the "International Tables for X-ray Crystallography".[17]

The structure of $Pt_2In_{14}Ga_3O_8F_{15}$ was solved in the space group $R\bar{3}m$ (by direct methods and refined against the F^2 data to residuals wR2 = 0.088 for all 1653 reflections, R1 = 0.054 for 1210 reflections with $I > 2\sigma(I)$) with anisotropic displacement parameters for all atoms (see Table 1, Table S1, and Table S2). The final refinement has been performed with a particular ordering of O and F, because this ordering is required according to bonding analysis (see below). That the chosen O/F ordering is reasonable is also indicated by lower R values of approximately 2% with respect to a refinement with the statistical distribution of O and F on all sites.

The thermal parameters of F(3) are highly anisotropic, i.e., U_{33} is approximately five times larger than U_{11} and U_{22} (Table S1). This suggests a displacement of F(3) along the c-axis, i.e., the 3-fold rotational axis of the $In(1)_6$ octahedron containing F(3) at the center, but no off-center position could be refined (see below). Furthermore, F(4) lies on a split position with half-occupancy as a consequence of the mirror plane perpendicular to the a-axis in $R\bar{3}m$. Although precession photographs clearly indicate that $Pt_2In_{14}Ga_3O_8F_{15}$ crystallizes in a trigonal rhombohedral space group with Laue group $\bar{3}m$, refinements in subgroups of $R\bar{3}m$ (e.g., $R\bar{3}$ or $R32$) under the inclusion of possible twinning did not give better results. Table 1 presents the final results for the refined atomic positions and isotropic displacement factors for $Pt_2In_{14}Ga_3O_8F_{15}$.[18]

Table 1. Positional Parameters and Isotropic Displacement Factors (pm^2) for $Pt_2In_{14}Ga_3O_8F_{15}$ [a]

atom	Wyckoff position	x	y	z	U_{iso}
Pt(1)	6*c*	1/3	2/3	0.0631(1)	0.0057(1)
In(1)	18*h*	0.1639(1)	0.3278(1)	0.0299(1)	0.0081(2)
In(2)	18*h*	0.9949(1)	0.4974(1)	0.0955(1)	0.0142(3)
In(3)	6*c*	0	0	0.1511(1)	0.0475(1)
Ga(1)	3*b*	0	0	1/2	0.0074(7)
Ga(2)	6*c*	2/3	1/3	0.0329(1)	0.0065(4)
O(1)	18*h*	0.8094(6)	0.6189(9)	0.0191(2)	0.009(1)
O(2)	6*c*	2/3	1/3	0.0740(3)	0.012(3)
F(1)	18*h*	0.8238(8)	0.6475(9)	0.1134(2)	0.034(3)
F(2)	6*c*	0	0	0.0544(3)	0.014(3)
F(3)	3*a*	0	0	0	0.009(4)
F(4)[b]	36*i*	0.1610(20)	0.2456(15)	0.4757(2)	0.028(5)

[a] The space group is $R\bar{3}m$, and the cell parameters are $a = 709.0(6)$ pm and $c = 4556.0(2)$ pm. [b] This position is only half-occupied.

2.3. Magnetic Susceptibility Measurement. The magnetic susceptibility of a sample of $Pt_2In_{14}Ga_3O_8F_{15}$ was measured using a SQUID susceptometer at a constant external magnetic field 5 T as a function of temperature. The measurements show that $Pt_2In_{14}Ga_3O_8F_{15}$ is diamagnetic with a susceptibility of -3.6×10^{-4} emu/mol. The latter is in reasonable agreement with the value expected from the diamagnetic contributions of the constituent atoms (O^{2-}, -12×10^{-6} emu/mol; F^-, 1.1×10^{-5} emu/mol; Ga^{3+}; -8×10^{-6} emu/mol; In^{3+}, -19×10^{-6} emu/mol; Pt^{4+}, -28×10^{-6} emu/mol).[19]

2.4. Electronic Structure Calculations. Self-consistent linear muffin-tin orbital (LMTO) electronic band structure calculations were performed using the program tight-binding LMTO Version 4.7.[20] Here, the density functional theory is used with the local density approximation in the form of the LMTO method in the atomic spheres approximation.[21] All k-space integrations were performed with the tetrahedron method using 320 k points within the Brillouin zone.[22] The basis sets consisted of 5s/5p orbitals for In, 4s/4p orbitals of Ga, 2s/2p orbitals for O and F, and 5d/6s/6p orbitals for Pt. The 5f orbitals of Pt, the 5d/4f orbitals of In, the 4d orbitals of Ga, and the 3s/3d orbitals of F and O were dealt with the down-folding technique,[23] treating the inner electrons as a soft core. The interatomic space was filled with interstitial empty spheres such that the overlap between adjacent spheres does not exceed 18%.

The electronic structures of the $PtIn_6$ cluster of $Pt_2In_{14}Ga_3O_8F_{15}$, the $RuSn_6$ cluster of $RuSn_6[(Al_{1/3-x}Si_{3x/4})O_4]_2$, and the $IrBi_6$, Bi_6 and Bi_5 clusters of $Bi_{34}Ir_3Br_{37}$ were calculated by extended Hückel tight-binding calculations.[24] The structures of the $PtIn_6$, $RuSn_6$, and $IrBi_6$ clusters were taken to be regular octahedra using the average metal−ligand bond lengths. In a similar manner, the structures of the Bi_6 and Bi_5 clusters of $Bi_{34}Ir_3Br_{37}$ were taken to have the O_h and C_{4v} point symmetry groups, respectively. The Ru 4d, Ir 5d, Pt 5d, In 5s/5p, Sn 5s/5p, and

(14) Buresch, O.; Schnering, H. G. v. *Fresenius' Z. Anal. Chem.* **1984**, *319*, 418.
(15) Sheldrick, G. M. *SHELXS-86*, Program for the Solution of Crystal Structures; University of Göttingen: Göttingen, Germany, 1986.
(16) Sheldrick, G. M. *SHELXL-97*, Program for the Refinement of Crystal Structures from Diffraction Data; University of Göttingen: Göttingen, Germany, 1997.
(17) Hahn, T., Ed. *International Tables of Crystallography*, Vol. A, 4th ed.; Kluwer: Dordrecht, The Netherlands, 1995.
(18) Further details of the crystal structure investigation may be obtained from the Fachinformationzentrum Energie, Physik, Mathematik, D-76344 Eggenstein-Leopoldshafen 2, on quoting the depository number CSD-414555, the names of the authors, and the journal citation.
(19) Selwood, P. W. *Magnetochemistry*, 2nd ed.; Interscience: New York, 1956.
(20) Andersen, O. K. *Program Tight-Binding LMTO*, Version 4.7; Stuttgart, Germany, 1994 (last update 2004).
(21) (a) Andersen, O. K. *Phys. Rev. B* **1975**, *12*, 3060. (b) Andersen, O. K.; Jepsen, O. *Phys. Rev. Lett.* **1984**, *53*, 2571. (c) Jepsen, O.; Andersen, O. K. *Z. Phys. B* **1995**, *97*, 35.
(22) Jepsen, O.; Andersen, O. K. *Solid State Commun.* **1971**, *9*, 1763.
(23) Jepsen, O.; Andersen, O. K. Snob, M. *Linearized Band-Structure Method in Electronic Band Structure and Its Applications*; Lecture Notes in Physics; Springer: Berlin, 1987.
(24) Our calculations were carried out by employing the SAMOA (Structure and Molecular Orbital Analyzer) program package (Dai, D.; Ren, J.; Liang, W.; Whangbo, M.-H. http://chvamw.chem.ncsu.edu/, 2002).

Table 2. Interatomic Distances (pm) of $Pt_2In_{14}Ga_3O_8F_{15}$

Pt−In(2)	254.8 (3×)	In(3)−F(4)	316.8 (3×)
Pt−In(1)	257.4 (3×)	In(3)−F(4)	334.6 (6×)
In(1)−O(1)	224.8 (2×)	In(3)−F(1)	368.0 (3×)
In(1)−O(1)	226.0	In(1)−In(1)	360.3 (2×)
In(1)−F(2)	230.4	In(1)−In(2)	364.4 (2×)
In(1)−F(3)	243.0	In(2)−In(2)	359.7 (2×)
In(2)−F(1)	213.5 (2×)	Ga(1)−F(4)	188.7 (6×)
In(2)−F(4)	222.8	Ga(2)−O(1)	186.1 (3×)
In(2)−O(2)	225.2	Ga(2)−O(2)	184.9
In(3)−F(1)	276.4 (3×)		

Bi 6s/6p orbitals were represented by double-ζ Slater type orbitals.[25] The atomic parameters used for calculations are summarized in Supplementary Information Table S3.

3. Crystal Structure

3.1. Local Coordination Environments. Initially, the distribution of O and F at the six different anion sites of $Pt_2In_{14}Ga_3O_8F_{15}$ was not straightforward, although there were some hints from the refinements. From the WDX analysis of single crystals and the synthesis of pure powder samples, it became clear that the O/F ratio should be close to 8:15.

The O/F ordering was determined by analyzing the Ga−F and Ga−O bond distances (Table 2). Ga(1) is coordinated by six F(4) with bond distances of 189 pm, which are comparable to those of other hexafluorogallates, e.g., 188−191 pm in Li_3GaF_6.[26] F(4) lies on a split position, and therefore two orientations of the GaF_6 octahedra are possible. The occupation of the F(4) anion site by O is unrealistic, because the resulting Ga−O distance of 189 pm would be much shorter than the typical Ga−O bond, e.g., Ga−O = 201.2 pm in the GaO_6 octahedra of Ga_2O_3.[27] Ga(2) is coordinated by three O(1) atoms and one O(2) atom with Ga−O distances of 186 and 185 pm, respectively, which lie within the range found for other *o*-gallates, e.g., $Li_3Na_2GaO_4$ and CsK_4GaO_4,[28] in which the Ga atoms are also four-coordinate. The occupation of the O(1) and one O(2) sites by F is not reasonable because this would result in unrealistically long Ga(2)−F distances. In addition, no fluorogallate with tetrahedrally coordinated Ga is known because Ga prefers to have a six-coordination with F. The F(1), F(2), and F(3) atoms are only connected to In. Under the assumption that these sites are 100% occupied by F atoms, the analytically determined ratio O/F = 8:15 is obtained.

As depicted in Figure 1, $Pt_2In_{14}Ga_3O_8F_{15}$ crystallizes in a new structure type, whose characteristic building units are $PtIn_6$ octahedra, GaF_6 octahedra, and GaO_4 tetrahedra. Each $PtIn_6$ octahedron consists of three In(1) (Pt−In = 254.8 pm) and three In(2) atoms (Pt−In = 257.4 pm). The short Pt−In distances are comparable to those found for the $PtIn_6$ octahedra in $PtIn_7F_{13}$ [12] (253.0 and 254.7 pm) and $PtIn_6Ga_2O_8$ [5] (253.5 pm) but are significantly shorter than those of intermetallic phases with six-coordinate Pt, e.g., $LaPtIn_3$[29] (Pt−In = 269 pm) and $Sr_2Pt_3In_4$[30] (Pt−In = 265 pm). The [$PtIn_6$] clusters are slightly elongated along the *c*-axis (i.e., along the 3-fold rotational axis of each [$PtIn_6$] octahedron) with In(1)−In(1) and In(2)−In(2) distances of 360 pm and In(1)−In(2) distances of 364 pm, which are only slightly longer than those in elemental In (325−338 pm).

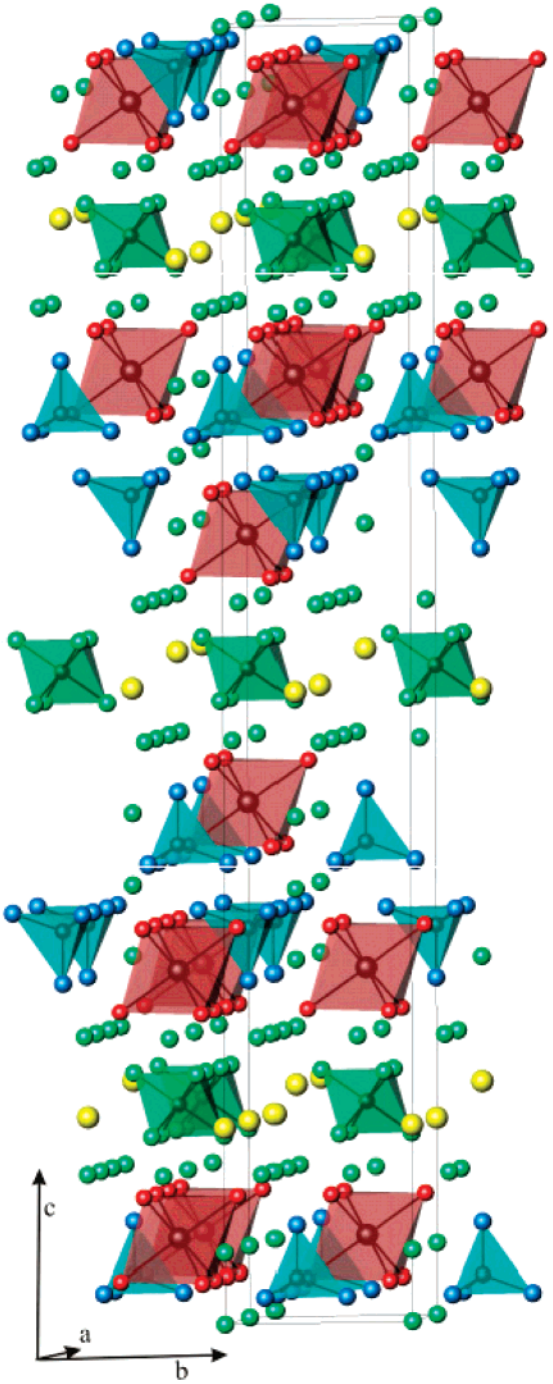

Figure 1. Perspective view of the crystal structure of $Pt_2In_{14}Ga_3O_8F_{15}$. The $[PtIn_6]^{10+}$ octahedra, $[GaF_6]^{3-}$ octahedral, and $[GaO_4]^{5-}$ tetrahedra are represented by red, green, and blue polyhedra, respectively. The green circles represent the F atoms, the blue circles the O atoms, and the yellow circles the In^+ ions.

Each In(1) is surrounded by one Pt, one F(1), one F(3), and three O(1) atoms, while each In(2) is surrounded by one Pt, one O(2), one F(4), and two F(1) atoms. Thus, as depicted in Figure 2, each $PtIn_6$ octahedron is surrounded by 12 O and 15 F atoms to form a $[PtIn_6]O_{12}F_{15}$ unit. In $PtIn_7F_{13}$ each $PtIn_6$ octahedron is surrounded by 24 F atoms. The high number (i.e., 27) of ligands around each $PtIn_6$ octahedron in $Pt_2In_{14}Ga_3O_8F_{15}$ can be understood because the ratio of the average In−In

(25) Clementi, E.; Roetti, C. *At. Data Nucl. Data Tables* **1974**, *14*, 177.
(26) Köhler, J.; Tyagi, A. K. *Z. Kristallogr.* **1999**, *214*, 25.
(27) Geller, S. *J. Chem. Phys.* **1960**, *33*, 676.
(28) (a) Köhler, J.; Hoppe, R. *Z. Anorg. Allg. Chem.* **1982**, *495*, 7. (b) Köhler, J.; Hoppe, R. *Z. Anorg. Allg. Chem.* **1984**, *511*, 201.
(29) Galadzhun, Y. V.; Pöttgen, R. *Z. Anorg. Allg. Chem.* **1998**, *625*, 481.
(30) Hoffmann, R.-D.; Pöttgen, R. *Z. Anorg. Allg. Chem.* **1998**, *625*, 994.

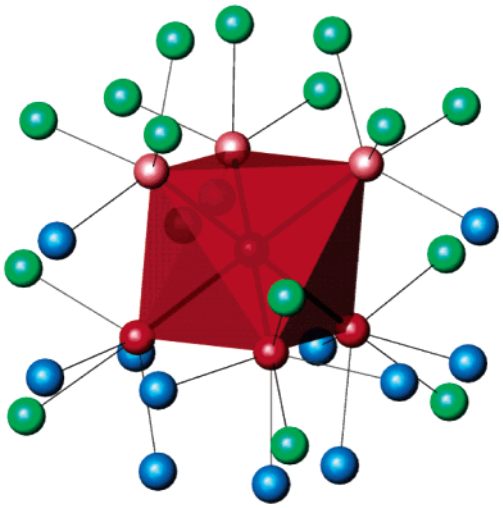

Figure 2. Perspective view of a $(PtIn_6)O_{12}F_{15}$ cluster in $Pt_2In_{14}Ga_3O_8F_{15}$. The $PtIn_6$ octahedron was highlighted by a polyhedral view. The dark red spheres correspond to the In(1) atoms, the light red spheres to the In(2) atoms, the green spheres to the F atoms, and the blue spheres to the O atoms.

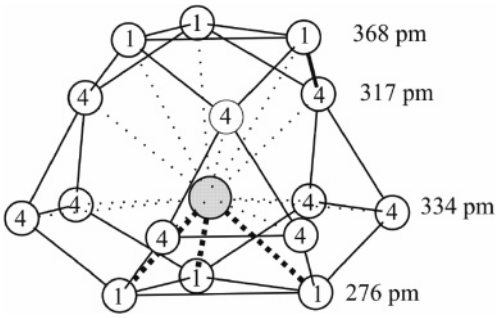

Figure 3. Perspective view of a $In(3)F_{15}$ polyhedron (point symmetry C_3) in $Pt_2In_{14}Ga_3O_8F_{15}$ together with the In(3)−F distances. In(3) is represented by a gray circle and the F by open circles.

distance to the average In−(O,F) distance is large (∼1.6). As a comparison, we note that each Nb_6 cluster of reduced oxoniobates has 18 O ligands, and the ratio of the Nb−Nb to the Nb−O average distance is ∼1.4. In clusters of the $M_6X_8X_6$ type (e.g., Nb_6I_{11} [31]), the M−M/M−X ratio is smaller (∼1.0), allowing for space only for 14 ligands around each M_6 octahedron.

In(3) is located in a large cage made up of 15 F atoms (Figure 3). The cage can be described as a distorted cuboctahedron in which one triangular face of three F(4) atoms is opened so that additional three F(1) atoms coordinate the In(3) atom with the In−F distance of 368 pm. Other In−F distances of this cage are 275 (×3), 317 (×3), and 334 (×6) pm. (For further discussion, see section 4.2.)

O(1) and O(2) are each tetrahedrally coordinated: one Ga(2) and three In(1) atoms around O(1) (Figure 4a) and one Ga(2) and three In(2) atoms around O(2) (Figure 4b**)**. Each F(1) lies in an In_3 triangle made up of one In(3) and two In(2) atoms with F−In(2) = 211.5 pm and F−In(1) = 274.8 pm. One additional In(3) lies above this triangle at the distance of 368 pm to F(3) (Figure 4c). Each F(2) atom is coordinated to three In(1) atoms to form a FIn_3 trigonal pyramid with F−In = 231 pm (Figure 4d). Each F(3) is located at the center of an $In(1)_6$ octahedron, all In atoms of which belong to different $PtIn_6$

(31) Simon, A.; Schnering, H. G. v.; Schäfer, H. *Z. Anorg. Allg. Chem.* **1967**, *355*, 195.

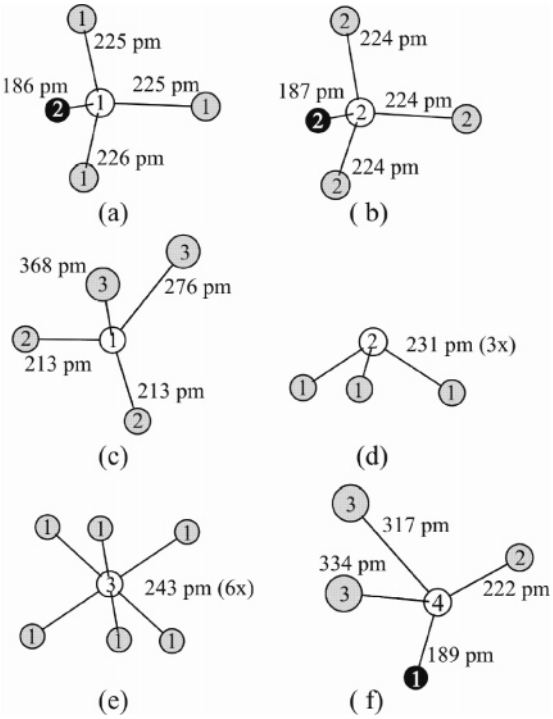

Figure 4. Schematic views of the coordination environments of (a) O(1), (b) O(2), (c) F(1), (d) F(2), (e) F(3), and (f) F4 atoms. Open circles correspond to O and F, respectively, gray circles to In, and black circles to Ga.

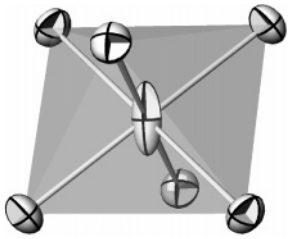

Figure 5. Perspective view of a $[F(3)In_6]$ octahedron where the thermal ellipsoid of F(3) is elongated along the 3-fold rotational axis of the octahedron parallel to the crystallographic *c*-axis. The thermal ellipsoids are represented with a factor of 3.94.

octahedra with a F−In distance of 243 pm (Figure 4e). However, its thermal parameters indicate an off-center position toward a triangular face of this octahedron, and as a result the real F−In distance should be slightly smaller than that calculated from the refined positional parameters (Figure 5). Finally, F(4) has a short bond of 189 pm to Ga(1) and is further surrounded by one In(2) and two In(3) (Figure 4f).

3.2. Highly Positive $[PtIn_6]^{10+}$ and Low-Valent In^+ Ions. The bond valence sum calculated for In(3) on the basis of its In−F bonds is 0.89.[32] It is therefore reasonable to assign the oxidation state +1 to the In(3) atoms. As shown in Figure 3, the environment of In(3) is highly anisotropic. The latter allows the mixing of the 5p orbitals into the 5s orbitals at In(3) to form a lone pair pointed in the direction of the more open space, thereby lowering its energy. The existence of low-valent In^+ in a highly ionic compound such as $Pt_2In_{14}Ga_3O_8F_{15}$ is remarkable because binary fluorides and oxides containing In atoms of oxidation state less than +3 are nearly unknown. All synthetic efforts to reduce InF_3 or In_2O_3 with hydrogen or elemental

(32) Brown, I. D.; Altermatt, D. *Acta Crystallogr.* **1985**, *B41*, 244.

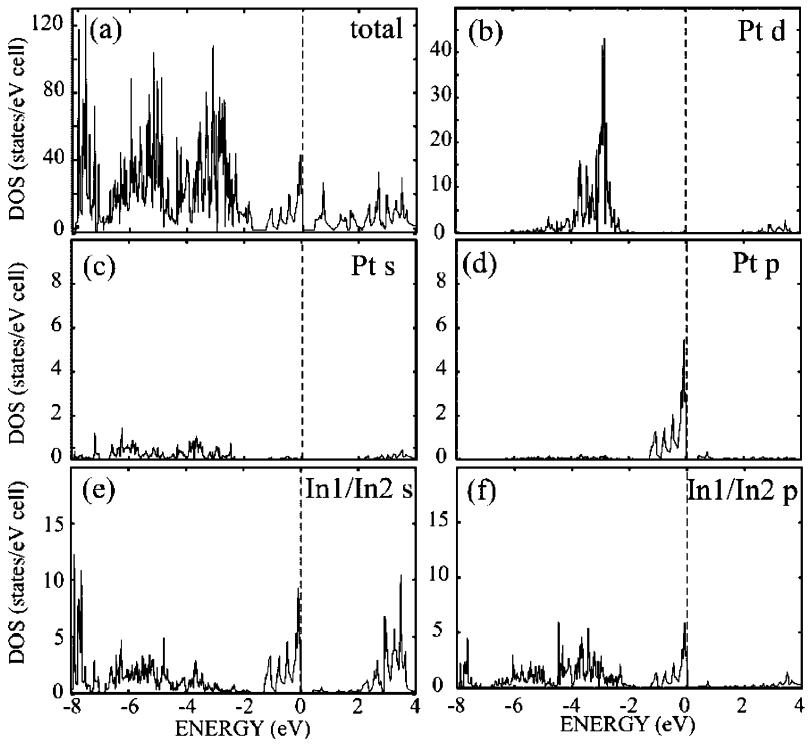

Figure 6. Electronic structure of $Pt_2In_{14}Ga_3O_8F_{15}$ obtained from LMTO calculations: (a) total DOS, (b) PDOS for the Pt 5d orbitals, (c) PDOS for the Pt 6s orbitals, (d) PDOS for the Pt 6p orbitals, (e) PDOS for the 5s orbitals of In(1) and In(2), and (f) PDOS for the 5p orbitals of In(1) and In(2). The Fermi level is indicated by a dashed line. The PDOS plots were calculated for one Pt, three In(1), and three In(2) atoms so as to represent the contributions from one $[PtIn_6]^{10+}$ cation.

indium, which date back to the 1930s,[33] were not successful. It has taken approximately 6 decades to discover $InBF_4$,[34] the first complex fluoride containing In^+. (The demarcation of a coordination sphere for a lone pair atom such as In^+ is often not straightforward. For example, one might ask whether only the three closest F(1) atoms with In−F = 276 pm should be counted as ligands. Although In^+ is a very large ion and comparable in size to Cs^+ or Tl^+, it should be mentioned that a high coordination number is usually found in intermetallic phases. Only in salts of the type $RbEu_3F_{10}$ [35] has a coordination number higher than 12 been observed.).

Using the oxidation states +3 for Ga, −2 for O, −1 for F, and +1 for In(3), the ionic electron counting for $Pt_2In_{14}Ga_3O_8F_{15}$ can be written as $([PtIn_6]^{10+})_2(In^+)_2([GaO_4]^{5-})_2[GaF_6]^{3-}(F^-)_9$. Namely, this electron counting places a charge of +10 on each $PtIn_6$ octahedron. In view of this high positive charge on a large $PtIn_6$ octahedron, it is in part understandable that as many as 27 anions (i.e., 12 O^{2-} and 15 F^- anions) surround each $[PtIn_6]^{10+}$ cation forming a $[PtIn_6]O_{12}F_{15}$ unit (Figure 2).

4. Electronic Structure

4.1. Electronic Band Structure of $Pt_2In_{14}Ga_3O_8F_{15}$. The plot of the total density of states (DOS) obtained for $Pt_2In_{14}Ga_3O_8F_{15}$ by LMTO calculations is presented in Figure 6a, which shows a band gap of approximately 0.4 eV. Given that $Pt_2In_{14}Ga_3O_8F_{15}$ is transparent and diamagnetic, one should expect a much larger band gap. This underestimation of the band gap is due to the well-known deficiency of DFT calculations.

The partial DOS (PDOS) plot calculated for the Pt 5d orbitals is shown in Figure 6b, that for the Pt 6s orbitals in Figure 6c, and that for the Pt 6p orbitals in Figure 6d. The d-block bands occur primarily in the region between −2 and −5 eV. The Pt 6s orbital contribution is substantial not only in the region of the d-block bands but also below the d-block bands (around −6 eV). The Pt 6p contribution occurs in the region immediately below the Fermi level and above the d-block bands (in the energy region of 0.0 to −1.8 eV).

The PDOS plot for the 5s orbitals of In(1) and In(2) is shown in Figure 6e, and that for the 5p orbitals of In(1) and In(2), in Figure 6f. The 5s orbital contribution is strong in the energy region between −1.8 and 0.0 eV, while the 5p orbital contribution in the same region is significantly weaker.

The PDOS plots shown above reveal that the 5d levels of Pt are practically all filled, hence suggesting the d^{10} electron count for Pt, i.e., the zero oxidation state for Pt. Furthermore, the populations of the Pt 6s and 6p orbitals are substantial, so that the formal oxidation state of Pt is negative. To understand this observation, it is necessary to examine the MO's of an isolated $[PtIn_6]^{10+}$ ion, which is discussed in the next section.

The PDOS plots for the In(3) atoms which are not part of the $PtIn_6$ octahedron are shown in Figure 7. The 5s orbital contribution of these atoms occurs mainly in the region between −4.5 and −4 eV, and the 5p orbital contribution lies well above 0.4 eV. That there is no significant 5s/5p orbital mixing indicates a negligibly small stereochemical activity of the lone pair of electrons of In(3), although the environment of In(3) is highly anisotropic.

The PDOS plots for the 2s/2p orbitals of the O and F atoms are not shown for simplicity. Their contributions to the total DOS occur mainly in the energy region well below ∼−4 eV.

(33) Hannebohn, O.; Klemm, W. *Z. Anorg. Allg. Chem.* **1936**, *269*, 2.
(34) Fitz, H.; Müller, B. G. *Z. Anorg. Allg. Chem.* **1997**, *623*, 579.
(35) Arbus, A.; Fournier, M. T.; Picaud, B.; Boulon, G.; Vedrine, A. *J. Solid State Chem.* **1980**, *31*, 11.

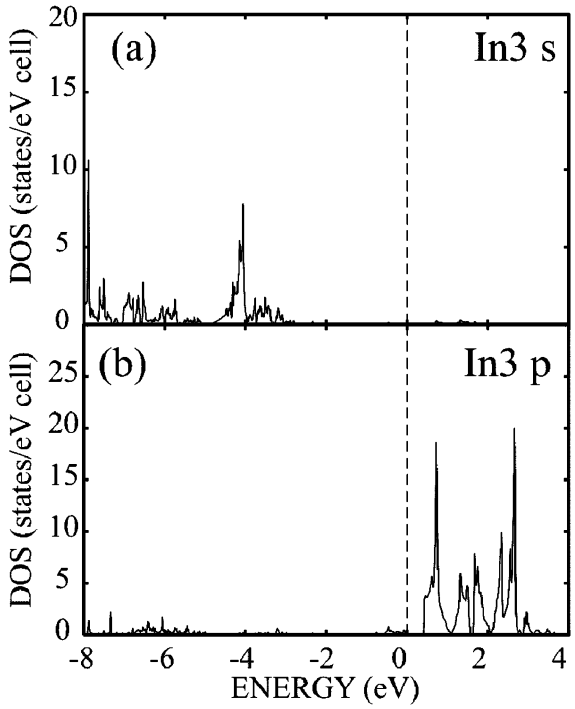

Figure 7. Electronic structure of $Pt_2In_{14}Ga_3O_8F_{15}$ obtained from LMTO calculations: (a) PDOS for 5s orbitals of In(3) and (b) PDOS for 5p orbitals of In(3). The Fermi level is indicated by a dashed line.

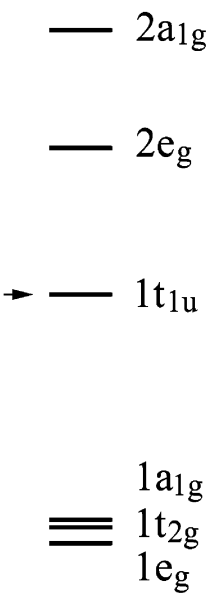

Figure 8. MO levels of the $[PtIn_6]^{10+}$ cation in $Pt_2In_{14}Ga_3O_8F_{15}$. The HOMO level is indicated by an arrow.

Thus, the oxidation assignments of −2 for O and −1 for F are justified, as expected.

4.2. Bonding and Oxidation State of Pt in a $[PtIn_6]^{10+}$ Octahedron. The essential features of the electronic band structure of $Pt_2In_{14}Ga_3O_8F_{15}$ discussed above are explained by the MO levels of an isolated $[PtIn_6]^{10+}$ ion presented in Figure 8. These MO levels are similar to those already reported in the study of $PtIn_7F_{13}$. In essence, these levels are largely made up of the Pt 5d/6s/6p and the In 5s orbitals. The linear combination of the six In 5s orbitals in the In_6 octahedron leads to the a_{1g}, t_{1u}, and e_g group orbitals,[36] while the Pt 5d orbitals are divided into the e_g and t_{2g} set. The a_{1g} group orbital of In_6 interacts

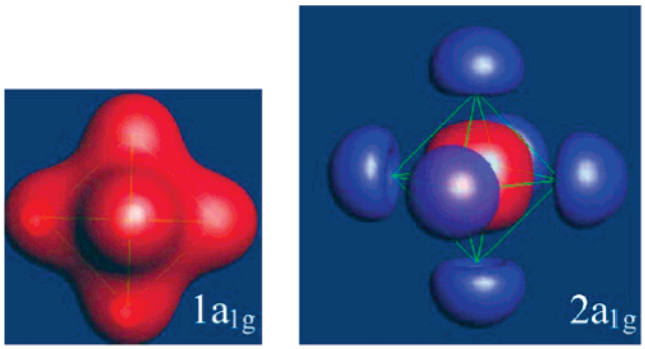

Figure 9. Boundary surface density plots calculated for the $1a_{1g}$ and $2a_{1g}$ levels of $[PtIn_6]^{10+}$.

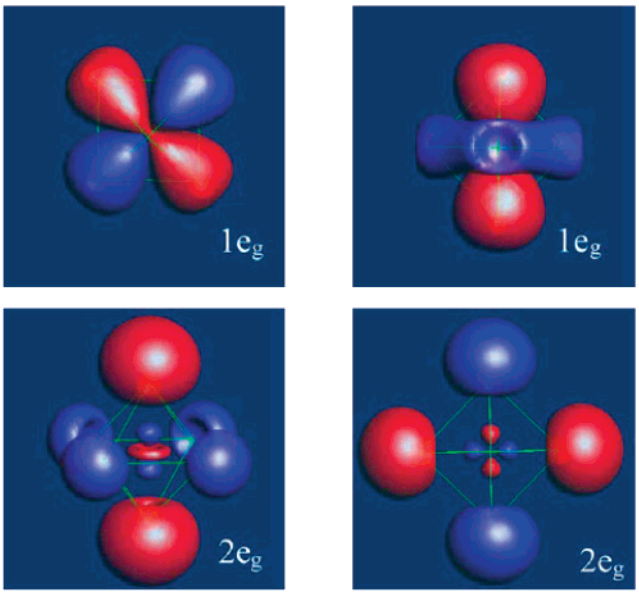

Figure 10. Boundary surface density plots calculated for the $1e_g$ and $2e_g$ levels of $[PtIn_6]^{10+}$.

with the 6s orbital of Pt, leading to the bonding level $1a_{1g}$ and the antibonding level $2a_{1g}$ (Figure 9). The $1e_g$ level has a greater contribution from the e_g orbitals of Pt, while the $2e_g$ level has a greater contribution from the e_g group orbitals of In_6 (Figure 10). The t_{1u} group orbitals of In_6 make bonding combinations with the Pt 6p orbitals to form the $1t_{1u}$ level of $[PtIn_6]^{10+}$ (Figure 11). The t_{2g} set of the Pt 5d orbitals make a weak bonding interaction with the 5p orbitals to form the $1t_{2g}$ level of $[PtIn_6]^{10+}$ (Figure 11).

The calculated MO levels increase in the order $1e_g$, $1t_{2g}$, $1a_{1g}$ < $1t_{1u}$ < $2e_g$. The $[PtIn_6]^{10+}$ ions have 18 valence electrons, so that the $1e_g$, $1t_{2g}$, $1a_{1g}$, and $1t_{1u}$ levels (nine altogether) are completely filled, while the $2e_g$ and $2a_{1g}$ levels are empty. The Pt 6s orbital contribution in the region of the d-block bands and below them originates from the $1a_{1g}$ orbitals of the $[PtIn_6]^{10+}$ ions. The DOS peaks of $Pt_2In_{14}Ga_3O_8F_{15}$ lying immediately above the d-block bands and below the Fermi level (between −1.8 and 0.0 eV) are related to the $1t_{1u}$ levels of the $[PtIn_6]^{10+}$ ions. These peaks occur because the symmetry of the $[PtIn_6]^{10+}$ ions is lower than the O_h point group and because $Pt_2In_{14}Ga_3O_8F_{15}$ has more than one $[PtIn_6]^{10+}$ ion per unit cell (i.e., six). The bottom portion (between 0.4 and 1.2 eV) of the

(36) Albright, T. A.; Burdett, J. K.; Whangbo, M.-H. *Orbital Interactions in Chemistry*; Wiley: New York, 1985.

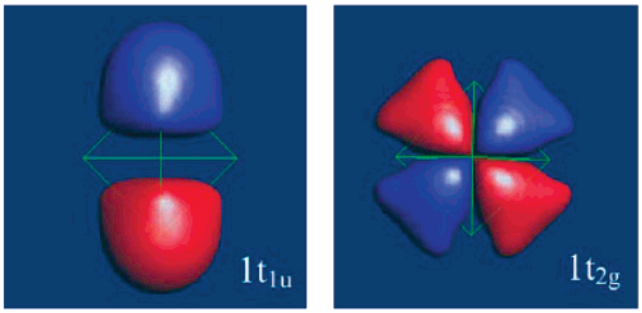

Figure 11. Boundary surface density plots calculated for one of the $1t_{1u}$ and $1t_{2g}$ orbitals of $[PtIn_6]^{10+}$. The $1t_{1u}$ and $1t_{2g}$ sets each have three degenerate orbitals. For simplicity, only one of the three is shown for each set.

conduction bands associated with the 5s orbitals of In(1) and In(2) originate from the empty $2e_g$ levels of the $[PtIn_6]^{10+}$ ions.

On the basis of the MO diagram of Figure 8, we consider the electron count and the oxidation state of Pt. For simplicity, suppose that the $1e_g$ level of $[PtIn_6]^{10+}$ is composed solely of the e_g level of Pt 5d and the $1a_{1g}$ level solely of Pt 6s. In this ionic electron counting, the electron count for Pt becomes $d^{10}s^2$, which implies the -2 oxidation state for Pt. As an alternative electron counting, we consider the effect of covalent bonding in $[PtIn_6]^{10+}$. In the $1a_{1g}$, $1e_g$, and $1t_{1u}$ levels of $[PtIn_6]^{10+}$, the Pt 6s, 5d, and 6p orbitals make bonding interactions with the group orbitals of In_6, respectively. From the viewpoint of covalent bonding, only half of the 12 electrons in these levels should be assigned to Pt. Therefore, these six electrons plus the six electrons of the $1t_{2g}$ level lead to 12 electrons on Pt, again suggesting the -2 oxidation state for Pt.

According to the above discussion, the Pt 5d orbitals can be considered as a reservoir for holding 10 electrons, and the essential bonding between Pt with its surrounding In ligands takes place by use of the 6s and 6p orbitals of Pt. In other words, the Pt atom of $[PtIn_6]^{10+}$ behaves like a main group element in its bonding with the In ligands. Such a picture of bonding was also reached in the electronic structure study of the highly negative anions $[MIn_{10}]^{10-}$ found in $K_{10}In_{10}M$ (M = Ni, Pd, Pt).[7] What is apparently surprising is that this bonding picture arises from the highly positive cation $[PtIn_6]^{10+}$. This picture is unusual from the conventional picture of bonding for transition metal elements, which is based on the interaction between an electropositive transition metal and electronegative main group elements. However, Pt is more electronegative than In,[37] and the In 5s level lies higher in energy than the Pt 5d level.[24] In such a case, the traditional ideas of positive oxidation states for transition metals and completely filled valence shells for main group ligands are not appropriate, as has been pointed out.[38] The report on the possible oxidation state -2 for Pt in the $[PtIn_6]^{10+}$ from the study of $PtIn_7F_{13}$ has stimulated the search for platinides. Indeed, the reaction of the electropositive metals Cs and Ba with Pt powder results in such compounds, e.g., BaPt,[39a] Cs_2Pt,[39b] and CsPt.[39c]

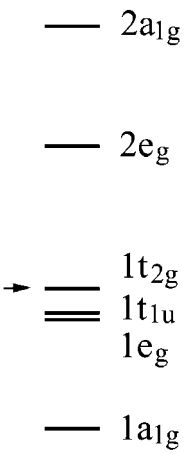

Figure 12. MO levels calculated for the $[RuSn_6]^{14+}$ ion of $RuSn_6[(Al_{(1/3)-x}Si_{3x/4})O_4]_2$. The HOMO level is indicated by an arrow.

5. Other Isolated Octahedral Clusters of Main Group Elements Stuffed with a Transition Metal Atom

In this section we examine other isolated octahedral cluster cations of main group elements stuffed with a transition metal atom, i.e., the $[RuSn_6]^{14+}$ cation of $RuSn_6[(Al_{1/3-x}Si_{3x/4})O_4]_2$ and the "$[IrBi_6]^{11+}$" cation of $Bi_{34}Ir_3Br_{37}$. The $[RuSn_6]^{14+}$ cation has 18 valence electrons as does $[PtIn_6]^{10+}$. The Mössbauer study of $RuSn_6[(Al_{1/3-x}Si_{3x/4})O_4]_2$ suggests that the Sn atoms are highly ionic and they differ from any Sn of known Sn-containing compounds.[4] If one were to assign the oxidation state $+2$ for the Sn of $[RuSn_6]^{14+}$, then the oxidation state for the Ru of $[RuSn_6]^{14+}$ would be $+2$ as well. The MO levels calculated for an isolated $[RuSn_6]^{14+}$ ion are depicted in Figure 12, which shows the orbital sequence $1a_{1g} < 1e_g$, $1t_{1u}$, $1t_{2g} < 2e_g < 2a_{1g}$. With 18 valence electrons, the levels up to $1t_{2g}$ are completely filled. The major orbital component of the $1t_{2g}$ level is given by the Ru 4d orbitals. Thus, the oxidation assignment of Sn^{2+} (s^2) and Ru^{2+} (d^6) requires that the major orbital component of the $1a_{1g}$, $1e_g$, and $1t_{1u}$ levels (six levels altogether) is given by the Sn 5s orbitals. However, the $1a_{1g}$, $1e_g$, and $1t_{1u}$ levels have substantial contributions from the Ru 5s, 4d, and 5p orbitals, respectively. Therefore, in the sense of covalent electron counting, half the electrons of the $1a_{1g}$, $1e_g$, and $1t_{1u}$ levels (i.e., six electrons) may be regarded as belonging to the Ru atom. These electrons plus the six electrons of the $1t_{2g}$ level lead to Ru^{4-} ($d^{10}s^2$) and hence Sn^{3+} (s^1). The true picture may lie between the ionic and covalent descriptions, i.e., close to the oxidation states of Ru^- (d^9) and $Sn^{2.5+}$ ($s^{1.5}$).

As already pointed out, $Bi_{34}Ir_3Br_{37}$ consists of three $IrBi_6$ octahedra, one Bi_6 octahedron, two Bi_5 square pyramids, and 37 Br atoms per formula unit. Ruck assigned the charge balance of $Bi_{34}Ir_3Br_{37}$ as $([IrBi_6]^{11+})_3([Bi_6]^{2+})([Bi_5]^+)_2(Br^-)_{37}$ and the oxidation state $+3$ for Ir. From experimental viewpoints, this assignment appears quite unreasonable because it suggests that Ir metal used as a starting material for the synthesis of $Bi_{34}Ir_3Br_{37}$ is oxidized by either Bi metal or $BiBr_3$. It is noted that Ir has a greater electronegativity than does Bi (i.e., 2.20 vs 2.02

(37) http://www.webelements.com/.
(38) (a) Paradis, J. A.; Whangbo, M.-H.; Kasowski, R. V. *New J. Chem.* **1993**, *17*, 525. (b) Lee, K.-S.; Koo, H.-J.; Dai, D.; Ren, J.; Whangbo, M.-H. *Inorg. Chem.* **1999**, *38*, 340. (c) Lee, K.-S.; Koo, H.-J.; Ren, J.; Whangbo, M.-H. *J. Solid State Chem.* **1999**, *147*, 11.
(39) (a) Köhler, J. Unpublished results. BaPt crystallizes in the NiAs type structure with space group = *P*63/*mmc*, *a* = 504.6 pm, *c* = 541.4 pm, Ba at (1/3, 2/3, 1/4), and Pt at (0, 0, 0). (b) Karpov, A. S.; Nuss, J.; Wedig, U.; Jansen, M. *Angew. Chem.* **2003**, *115*, 4966; *Angew. Chem., Int. Ed.* **2003**, *42*, 4818. (c) Powder samples of CsPt are characterized by X-ray powder diffraction data. The observed *d*-values (intensities) are 6.19 (65), 3.24 (10), 3.09 (100), 2.68 (10), 2.46 (10), 2.22 (50), 2.06 (20), 2.05 (30), 1.94 (20), 1.90 (5), 1.81 (5), 1.73 (20), 1.63 (15), 1.54 (20), 1.44 (10), 1.35 (10), 1.32 (20), 1.29 (20), 1.21 (15), 1.14 (10), and 1.14 (10). The indexing and the structure determination have not yet been successful.

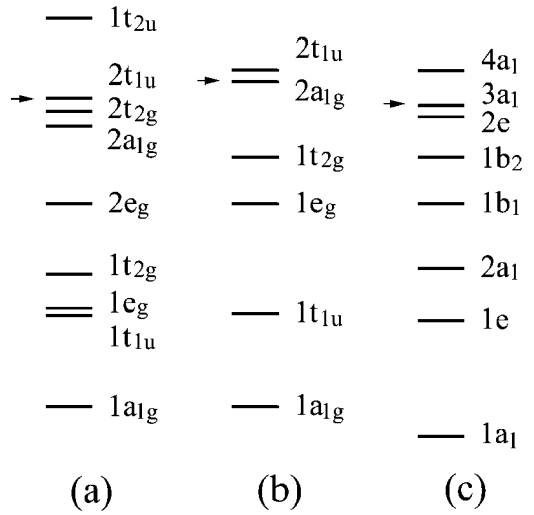

Figure 13. MO levels calculated for the (a) $[IrBi_6]^{3+}$, (b) $[Bi_6]^{10+}$, and (c) $[Bi_5]^{7+}$ ions of $Bi_{34}Ir_3Br_{37}$. The HOMO levels are indicated by arrows.

in Pauling scale). According to our discussion of $[RuSn_6]^{14+}$ and $[PtIn_6]^{10+}$, a positive oxidation state for Ir would be inappropriate for $IrBi_6$. To estimate the overall charge on the $IrBi_6$ cluster and the oxidation state of Ir, we examine the MO levels of the $IrBi_6$, Bi_6 and Bi_5 clusters, which are presented in Figure 13. It is reasonable to assume that the MO levels of these clusters can be filled up to the bonding levels that are constructed from the Bi 6p orbitals, as depicted in Figure 13 (i.e., up to the $2t_{1u}$ level in $IrBi_6$, up to the $2a_{1g}$ level in Bi_6, and up to the $3a_1$ level in Bi_5). This gives rise to $[IrBi_6]^{3+}$, $[Bi_6]^{12+}$, and $[Bi_5]^{7+}$ ions. However, these cations do not balance the charge of $Bi_{34}Ir_3Br_{37}$. Among the three cations, the highest lying HOMO is found in $[Bi_6]^{10+}$ (i.e., $2a_{1g}$), and the next highest lying HOMO in $[IrBi_6]^{3+}$ (i.e., $2t_{1u}$). Therefore, the charge balance of $Bi_{34}Ir_3Br_{37}$ can be written as $([IrBi_6]^{4+})_2([IrBi_6]^{3+})([Bi_6]^{12+})$-$([Bi_5]^{7+})_2(Br^-)_{37}$. To estimate the oxidation state of Ir in Bi_{34}-Ir_3Br_{37}, it is necessary to examine the nature of the occupied MO's of $[IrBi_6]^{n+}$ ($n = 3, 4$).[40] The $2t_{1u}$ level is solely made up of the Bi 6p orbitals, while the $2t_{2g}$ level is largely made up of the Bi 6p orbitals. The $1a_{1g}$, $1t_{1u}$, and $1e_g$ levels (six levels altogether) are largely made up of the Bi 6s orbitals. The $1t_{2g}$ and $2e_g$ are largely made up of the Ir 5d orbitals, while the $2a_{1g}$ level has a large contribution form the Ir 6s orbital. To a first approximation,therefore, the Ir of $[IrBi_6]^{4+}$ or $[IrBi_6]^{3+}$ has the electron count close to $d^{10}s^2$ and hence the oxidation state close to -3.

(40) The bottom six levels of $IrBi_6$ (i.e., $1a_{1g}$, $1t_{1u}$, and $1e_g$) are largely composed of the Bi 6s orbitals; so are the bottom six levels of Bi_6 (i.e., $1a_{1g}$, $1t_{1u}$, and $1e_g$) and the bottom five levels of Bi_5 (i.e., $1a_1$, 1e, $2a_1$, and $1b_1$). There are three bonding levels solely made up of the Bi 6p orbitals in Bi_6 (i.e., $1t_{2g}$) and in Bi_5 (i.e., $1b_2$ and 2e). The $2t_{2g}$ and $2t_{1u}$ levels of $IrBi_6$ are similar in nature to the $1t_{2g}$ and $2t_{1u}$ levels of Bi_6, respectively.

The above discussion suggests that the oxidation states of the transition metal atoms in the $[RuSn_6]^{14+}$ and $[IrBi_6]^{n+}$ ($n = 3, 4$) cations are negative. This observation is entirely analogous to that already discussed for $[PtIn_6]^{10+}$. A similar finding is expected for octahedral clusters of rare-earth elements stuffed with transition metal atoms. For example, the electronic band structures of Pr_3I_3Ru and Y_3I_3Ru, which consist of condensed octahedral RE_6Ru (RE = Pr, Y) clusters, show that the d-block bands of Ru lie well below the Fermi level; i.e., they are completely filled.[41] The latter implies the d^{10} electron count for Ru and hence a negative oxidation state for Ru in these halides.

6. Concluding Remarks

The new oxyfluoride $Pt_2In_{14}Ga_3O_8F_{15}$ contains highly positive $[PtIn_6]^{10+}$ ions as well as low-valent In^+ ions. Our study indicates that the oxidation states of the transition metal atoms in the stuffed octahedral cluster cations $[PtIn_6]^{10+}$, $[IrBi_6]^{n+}$ ($n = 3, 4$), and $[RuSn_6]^{14+}$ are most probably negative rather than positive. For a compound of transition metal M coordinated by main group ligands L, this finding is highly unusual from the viewpoint of the conventional picture that the valence shells of L are completely filled and the oxidation state of M is positive. However, this picture is valid only when the transition metal M is more strongly electropositive than the ligand L, and hence the valence p-orbital of L lies lower in energy than the valence d-orbital of M. The conventional picture becomes inappropriate when the valence s-orbital of L lies higher than the valence d-orbital of M (e.g., $[PtIn_6]^{10+}$) or when the valence p-orbital of L lies considerably higher than the valence d-orbital of M (e.g., $[RuSn_6]^{14+}$ and $[IrBi_6]^{n+}$ ($n = 3, 4$)).

Acknowledgment. The authors thank R. Ramlau for the WDX analysis and E. Brücher for the measurement of the magnetic susceptibility and O. Jepsen for help with the LMTO program. M.-H.W. thanks the Office of Basic Energy Sciences, Division of Materials Sciences, U. S. Department of Energy, for financial support under Grant DE-FG02-86ER45259. This work is dedicated to Professor A. Simon on the occasion of his 65th birthday.

Supporting Information Available: Table S1 listing the crystallographic data and parameters of data collection and structure refinements of $Pt_2In_{14}Ga_3O_8F_{15}$, Table S2 giving the anisotropic displacement factors for $Pt_2In_{14}Ga_3O_8F_{15}$, and Table S3 showing the atomic parameters used for the EHTB calculations. This material is available free of charge via the Internet at http://pubs.acs.org.

JA044389S

(41) Köckerling, M.; Martin, J. D. *Inorg. Chem.* **2001**, *40*, 389.